IOPscience iopscience.iop.org

Home Search Collections Journals About Contact us My IOPscience

Remanence enhancement in nano-structured composite magnets

This article has been downloaded from IOPscience. Please scroll down to see the full text article.

1999 J. Phys.: Condens. Matter 11 3323

(http://iopscience.iop.org/0953-8984/11/16/013)

View the table of contents for this issue, or go to the journal homepage for more

Download details:
IP Address: 171.66.16.214
The article was downloaded on 15/05/2010 at 07:19

Please note that terms and conditions apply.

J. Phys.: Condens. Matter **11** (1999) 3323–3334. Printed in the UK PII: S0953-8984(99)99617-0

Remanence enhancement in nano-structured composite magnets

G P Zhao, H S Lim, C K Ong and Y P Feng
Department of Physics, National University of Singapore, 119260, Singapore

Received 24 November 1998, in final form 1 March 1999

Abstract. The remanence of an isotropic nanocrystalline exchange-coupled composite system (comprising hard and soft magnetic phases) is investigated analytically within a simple (one-dimensional) micromagnetic model, in which only exchange and anisotropy energies are considered. For a soft grain with size much less than its own Bloch wall width, our analysis shows that the magnetization distribution in the soft phase is linearly dependent upon position, which we show is responsible for the significant enhancement observed in composite systems. Furthermore, we show that a good estimate of the remanence can be provided by a simple formula, which is easily calculated by hand.

1. Introduction

The rare-earth–iron and rare-earth–cobalt magnetic materials are widely regarded as possibly the best available permanent magnetic materials because they possess the largest coercivity and thus the greatest energy product [1]. One drawback, however, is that these materials are chemically active and rather expensive to produce. Moreover, the saturation magnetizations M_S of these materials are generally much lower than those of soft magnetic materials. To further increase the energy product, an exchange-coupled composite material is proposed, with the hard phase to provide high coercivity and the soft phase to provide high saturation M_S and remanence M_r. These new materials are not only less expensive, but also less active as a result of a larger volume fraction of the relatively cheap soft magnetic materials, which envelop the hard phase.

The quality of these new materials depends largely on the microstructure. There have been many numerical and analytical studies of the influence of the microstructure of the composite materials on their magnetic properties [2–7]. While the numerical work can deal with more complicated problems, the analytical studies can often yield better insights into the physical understanding of the underlying phenomenon. To enable an analytical solution to be carried out, such studies often assume the presence of special easy-axis directions (which are normal to the applied field), although it has been found that the easy-axis orientations are random in many experimental studies [8–18]. In our work, we shall relax this restriction and show that an analytical solution is possible if we make some simplifying but reasonable assumptions about the remanent state.

The analytical modelling of remanence enhancement for single-phased magnetic materials has already been presented in reference [19]. In the present work, we concentrate on remanence enhancement of composite materials. The approach that we adopt may provide some insights into the phenomenon of remanence enhancement in composite magnetic systems.

0953-8984/99/163323+12$19.50 © 1999 IOP Publishing Ltd

2. The analytical model

The analytical model is a chain of rectangular nano-grains with soft-phase α-Fe grains and hard-phase (e.g. $Nd_2Fe_{14}B$) grains arranged alternatively, with the crystal easy axis varying from grain to grain. As a first step we shall deal with a triple-grain system shown in figure 1 with a soft-phased α-Fe grain enclosed by two hard-phased grains.

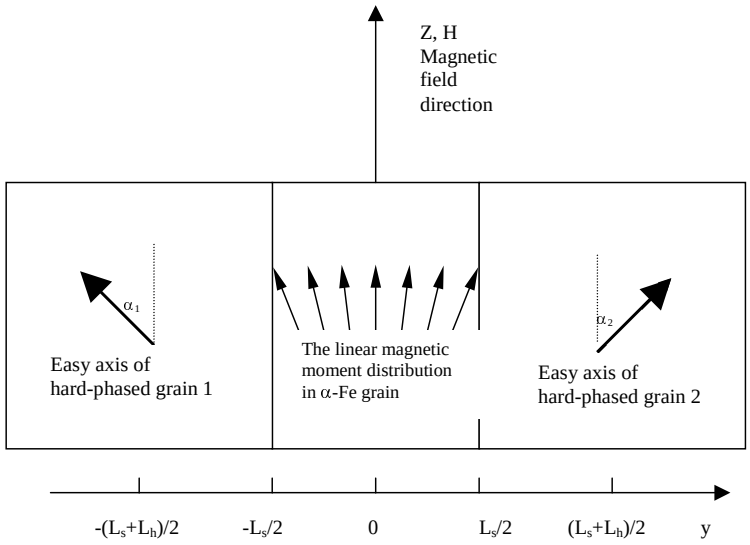

Figure 1. A magnetically soft grain (α-Fe) framed by two hard magnetic grains (e.g. $Nd_2Fe_{14}B$). The applied magnetic field $\boldsymbol{H}$ and the two easy axes of the hard grains lie in the same plane. The magnetic moment orientations in the α-Fe grain lie between two easy-axis directions $\boldsymbol{\alpha}_1$ and $\boldsymbol{\alpha}_2$, and change linearly with y.

The magnetic field is applied along the z-direction. For simplicity, the magnetization distribution is assumed to be uniform over the x–z plane. Furthermore, the easy axes of the hard grains and the magnetic moments will be restricted to the same y–z plane. This approach has effectively reduced the problem to a one-dimensional one, in which a plane-isotropic easy-axis distribution is assumed.

The one-dimensional distribution of the magnetic moment in equilibrium states can be found from the variation of the Gibbs free energy G of the system:

$$\delta G \equiv \delta \int g \, \mathrm{d}v = 0 \tag{2.1}$$

where g is the volume density of the Gibbs free energy. Normally g consists of four terms, namely, the exchange energy, the anisotropy energy, the stray field, and the magnetostatic energy of the magnetization in an applied field.

In our present work, we investigate the remanent magnetization of nanocrystalline composite materials. The grains are initially magnetized in the positive z-axis direction (see figure 1), and the field is reduced to zero after the magnetization. Since the applied magnetic field is zero in the remanent state, the magnetostatic energy term vanishes. The stray-field energy, on the other hand, is an important term expressing the long-range magnetostatic interaction that can affect the actual magnetization distribution. However, for rare-earth nanocrystalline composite materials, this interaction plays a less pivotal role in remanence

enhancement compared to the exchange interactions [4, 6, 7, 19]. In fact, it is conceivable to attribute the remanence enhancement entirely to intergrain exchange interactions. Thus, for the sake of simplicity, this term will henceforth be omitted from further discussion. Consequently, g contains only two terms, namely, the exchange energy and the anisotropy energy:

$$g = A(\nabla\theta)^2 + K\sin^2(\theta - \alpha) \tag{2.2}$$

where A denotes the exchange energy constant, K is the anisotropy constant, θ is the angle between the magnetization and the applied field (z-axis), and α is the angle between the easy axis and the applied field (figure 1). In our model, the easy-axis distribution is plane isotropic; in the remanent state, α is a random number varying from $-\pi/2$ to $\pi/2$ [19].

The variation of the Gibbs energy functional leads to two independent equations. The variation of the volume part results in the well-known Euler–Lagrange equation, which, in one dimension, can be written as

$$\frac{\partial g}{\partial \theta} = \frac{\mathrm{d}}{\mathrm{d}y}\left[\frac{\partial g}{\partial(\mathrm{d}\theta/\mathrm{d}y)}\right]. \tag{2.3}$$

The variation of the surface contributions to the energy, on the other hand, results in the Carl–Weierstrass relation. In any surface of the magnetic material, this relation has to be fulfilled. In one dimension, this boundary condition may be written as

$$A\frac{\mathrm{d}\theta}{\mathrm{d}y} = \text{constant}. \tag{2.4}$$

For composite materials with different exchange constants, this relation is important for the grain boundary. In our model, for instance, the boundary condition (equation (2.4)) leads to the discontinuity of the first derivative of θ with respect to y in the grain boundary (cf. figure 2(a)). Using equations (2.2), (2.3), and (2.4), we can now determine the direction of magnetization for each spatial point of the magnetic system.

3. The distribution of the magnetization and differential remanence enhancement

Since the exchange interaction is limited to neighbouring grains only, we first consider a linear chain of three grains with one soft-phased grain enclosed by two hard-phased grains (see figure 1). The remanence of a magnetic system is obtained by averaging this remanence over the whole volume. To calculate the remanence of a three-grain system, the first step is to determine the distribution of the magnetization within this system.

Table 1. Material parameters taken from reference [5]. M_S, K, A, and $\pi\Delta$ are the saturation magnetization, anisotropy constant, exchange energy constant, and the Bloch wall width, respectively.

Material	M_S (T)	K (10^6 J m^{-3})	A (10^{-12} J m^{-1})	$\pi\Delta$ (nm)
$Nd_2Fe_{14}B$	1.61	4.3	7.7	4.2
$Sm_2(Fe_{0.8}Co_{0.2})_{17}N_{2.8}$	1.55	10.1	4.8	2.2
$SmCo_5$	1.06	17.1	12.0	2.6
α-Fe	2.15	0.046	25.0	73.2

As shown in figure 1, the soft magnetic grain is bounded by $-L^s/2 < y < L^s/2$, where L^s denotes the average size of the soft grain. Furthermore, from the viewpoint of symmetry, we only consider the region defined by $-(L^s + L^h)/2 < y < (L^s + L^h)/2$, so the magnetic system studied consists of one soft grain and two halves of the hard grains. The superscripts s and h denote soft and hard, respectively. Considering that the anisotropy of the hard-phased material

(e.g. $Nd_2Fe_{14}B$) is about two orders of magnitude larger than that of the soft-phased material (see table 1), a further simplification can be made by ignoring the anisotropy energy of the soft phase. Physically, this simplification means that the magnetization within the soft-phased grain is completely determined by the exchange hardening of neighbouring hard grains. This assumption is valid provided that the size of the soft grain is smaller than half of the Bloch wall width [4]. For α-Fe, this critical grain size is 36.6 nm (table 1). Studies have shown that significant remanence enhancement can only be obtained with a soft-grain size less than this value [9, 14–17]. The magnetization at the centre of a hard-phased grain, however, is determined by the Stoner–Wohlfarth (S–W) model, according to which the magnetic moments orient themselves along the easy-axis direction in the remanent state. For a hard grain with a size several times larger than its own Bloch wall width, the magnetization near the grain centre is unaffected by the neighbouring grains' magnetic moment orientations.

With these assumptions, the volume density of the energy of the system under consideration can be written as

$$g = \begin{cases} A^s \left(\dfrac{\mathrm{d}\theta}{\mathrm{d}y}\right)^2 & \text{for } |y| \leqslant L^s/2 \\ A^h \left(\dfrac{\mathrm{d}\theta}{\mathrm{d}y}\right)^2 + K^h \sin^2(\theta - \alpha) & \text{for } L^s/2 \leqslant |y| \leqslant (L^s + L^h)/2. \end{cases} \tag{3.1}$$

Using equation (2.3), we obtain the following expressions for the Euler–Lagrange equations:

$$A^s \frac{\mathrm{d}^2\theta}{\mathrm{d}y^2} = 0 \tag{3.2}$$

$$2A^h \frac{\mathrm{d}^2\theta}{\mathrm{d}y^2} = K^h \sin 2(\theta - \alpha) \tag{3.3}$$

for soft- and hard-phased regions respectively. Multiplying equations (3.2) and (3.3) with $\mathrm{d}\theta/\mathrm{d}y$, we obtain, after a subsequent partial integration,

$$A^s \left(\frac{\mathrm{d}\theta}{\mathrm{d}y}\right)^2 = C^s \tag{3.4}$$

$$A^h \left(\frac{\mathrm{d}\theta}{\mathrm{d}y}\right)^2 = K^h \sin^2(\theta - \alpha) + C^h \tag{3.5}$$

where C^s and C^h are the integration constants, which can be deduced from the boundary conditions. The boundary conditions include the Carl–Weierstrass relation given by equation (2.4) at both $y = -L^s/2$ and $y = L^s/2$, as well as the infinite-boundary condition. The latter condition indicates that at places infinitely removed from the grain boundary, the orientations of the magnetic moments are totally determined by the S–W model. Since the grain size is finite, the magnetic moment furthest from the grain boundary is located at the grain centre. Thus, we arrive at the following boundary conditions:

$$\theta = \alpha_1 \text{ and } \frac{\mathrm{d}\theta}{\mathrm{d}y} = 0 \qquad \text{for } y = -(L^s + L^h)/2 \tag{3.6}$$

$$\theta = \alpha_2 \text{ and } \frac{\mathrm{d}\theta}{\mathrm{d}y} = 0 \qquad \text{for } y = (L^s + L^h)/2. \tag{3.7}$$

One can infer from equations (3.6) and (3.7) that C^h in equation (3.5) should be zero. Equations (2.4) and (3.4)–(3.7) are then solved to give the following distributions of the magnetic moment orientations,

$$\tan\left(\frac{\alpha_2 - \theta}{2}\right) = \tan\left(\frac{\alpha_2 - \alpha_1 - \delta^s}{4}\right) \exp\left[-(y - L^s/2)/\Delta^h\right] \qquad \text{for } y > L^s/2 \tag{3.8}$$

$$\tan\left(\frac{\theta-\alpha_1}{2}\right)=\tan\left(\frac{\alpha_2-\alpha_1-\delta^s}{4}\right)\exp\left[(y+L^s/2)/\Delta^h\right] \qquad \text{for } y<-L^s/2 \qquad (3.9)$$

$$\theta=\frac{\alpha_1+\alpha_2}{2}+\frac{y}{L^s}\delta^s \qquad \text{for } |y|<L^s/2 \qquad (3.10)$$

where

$$\Delta^h=\sqrt{A^h/K^h}$$

is the exchange length [6, 7] of the hard phase, $\delta^s=\theta_2-\theta_1$, and the quantity $\pi\Delta^h$ gives the Bloch wall width of a 180° domain wall of a hard-phased material. θ_1 and θ_2 are the magnetic moment orientations in the grain boundaries at $y=-L^s/2$ and $y=L^s/2$, respectively. Using equation (3.5), the gradient of the magnetic moment orientation θ in the hard-phased region is given by

$$\left(\frac{\mathrm{d}\theta}{\mathrm{d}y}\right)^h=\pm\sqrt{\frac{K^h}{A^h}}\sin(\theta_b-\alpha) \qquad (3.11)$$

where θ_b is continuous in the grain boundaries. It follows from equation (3.10) that

$$\theta_b=(\alpha_1+\alpha_2\pm\delta^s)/2.$$

Since the distribution of the magnetic moment orientations in the soft-phased region is linear (cf. equation (3.10)), we may write for the grain boundaries $(\mathrm{d}\theta/\mathrm{d}y)^s=\delta^s/L^s$.

Using the preceding results, the Carl–Weierstrass relation (equation (2.4)) can thus be expressed as

$$\delta^s=\frac{L^s}{L_{\mathrm{ex}}}\sin\left[\frac{1}{2}(\alpha_2-\alpha_1-\delta^s)\right] \qquad (3.12)$$

where

$$L_{\mathrm{ex}}=A^s/\sqrt{A^hK^h}=A^s\Delta^h/A^h$$

denotes the length of exchange hardening of the soft grains with the neighbouring hard magnetic grains. Equation (3.12) indicates that δ^s increases with both L^s and the angle $\alpha_2-\alpha_1$, while it decreases with L_{ex}. The larger L_{ex}, the smaller δ^s, and the greater the effect of the exchange hardening, which leads to larger remanence enhancement. For α-Fe bounded by $Nd_2Fe_{14}B$, $Sm_2(Fe_{0.8}Co_{0.2})_{17}$, or $SmCo_5$ (see table 1), the corresponding L_{ex}s are given by 4.34 nm, 3.59 nm, and 1.75 nm, respectively. Thus, for a given soft-grain (α-Fe) size, remanence enhancement would be most effective if we had used $Nd_2Fe_{14}B$ as the hard phase.

In the hard-phased grains, equations (3.8) and (3.9) show that $\theta-\alpha$ is exponentially decreasing with $y-L^s/2$, suggesting that the magnetic orientations are largely aligned along the easy-axis direction unless the magnetic moment is very near the grain boundary. Besides contributing little to the enhancement, the underlying mechanism is also similar to that operating within the single-phased system [19]. In contrast, equation (3.10) indicates that, in the soft-phased region, the distribution of the magnetic moment orientations is *linear*, which we will show is mainly responsible for the significant enhancement in the composite system.

The remanence of the soft grain is given by

$$M_r^s=\frac{M_S^s}{L^s}\int_{-L^s/2}^{L^s/2}\cos\theta\,\mathrm{d}y \qquad (3.13)$$

where the subscript S denotes saturation (so M_S^s means saturation magnetization of the soft grain). Using equation (3.10), we get

$$M_r^s=M_S^sL^s\frac{\sin(\delta^s/2)}{\delta^s/2}\cos\left(\frac{\alpha_1+\alpha_2}{2}\right). \qquad (3.14)$$

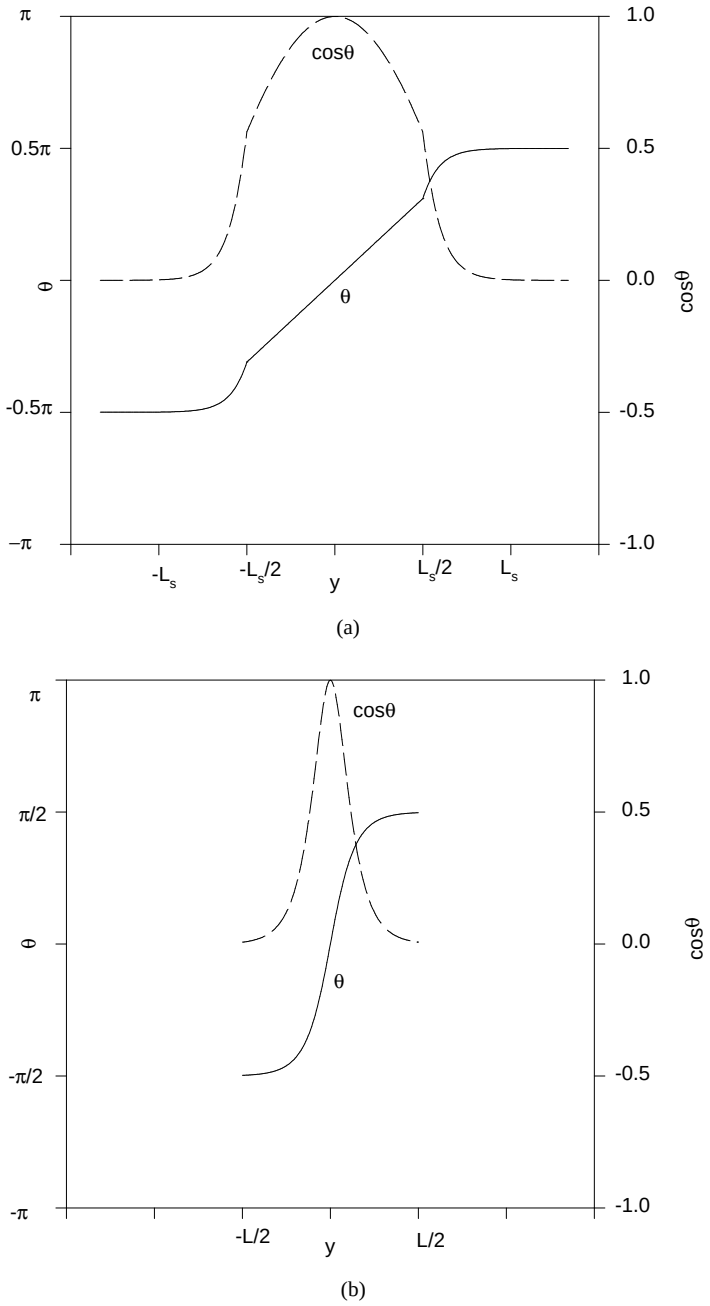

Figure 2. (a) The direction θ of the magnetic moment orientation and its projection $\cos\theta$ onto the applied-field direction. The calculations are done using Nd–Fe–B as the hard phase and assuming that the easy axes are given by $\alpha_1 = -\pi/2$ and $\alpha_2 = \pi/2$. (b) The results for single-phased Nd–Fe–B grains [19] are also shown for comparison. In this case, however, the grain boundary is located at $y = 0$ rather than at $y = \pm L/2$.

For sufficiently small L^s, δ^s can be made small enough (see equation (3.12)) that

$$\sin(\delta^s/2)/(\delta^s/2) \approx 1$$

thereby reducing equation (3.14) to

$$M_r^s \approx M_S^s L^s \cos\left(\frac{\alpha_1 + \alpha_2}{2}\right) \qquad \text{for small } L^s. \tag{3.15}$$

This means that all magnetization moments in the small soft grain are oriented in the direction given by $\theta = (\alpha_1 + \alpha_2)/2$.

We know that the mechanism of remanence enhancement for exchange-coupled single-phased grains is due to exchange interactions, which drive the magnetic moments in the grain boundaries away from the easy-axis directions [19]. This results in a larger enhancement for a system of small grains that exhibit a large difference in orientations between the neighbouring easy-axis directions. This conclusion is also valid for the exchange-hardened composite grains. Equation (3.12) shows that δ^s increases with L^s but is independent of the hard-grain size L^h. For fixed α_1 and α_2, the smaller δ^s, the larger the remanence enhancement. Thus for exchange-hardened composite grains, remanence enhancement increases with decreasing grain size L^s of the soft phase. In addition, equations (3.10) and (3.12) indicate that remanence enhancement increases with $\alpha_2 - \alpha_1$, and the largest remanence enhancement occurs when $\alpha_1 = -\pi/2$ and $\alpha_2 = \pi/2$.

For α-Fe grains enclosed by $Nd_2Fe_{14}B$ magnetic grains, the distributions of θ and $\cos\theta$ in the composite system are shown in figure 2(a) for $\alpha_1 = -\pi/2$ and $\alpha_2 = \pi/2$. The results [19] for the single-phased Nd–Fe–B grains are also shown for comparison in figure 2(b). We see that $\cos\theta$ is nearly 0 in the hard-phased region while it is much larger in the soft-phased grain. For isolated grains of the same easy-axis combination, the reduced remanence is always zero ($\cos(-\pi/2) = \cos(\pi/2) = 0$).

On closer inspection of figures 2(a) and 2(b), one can make the following interesting observation. As far as remanence enhancement is concerned, the soft grain in the composite system functions similarly to the grain boundaries in the single-phased system. The magnetization in the soft grain changes linearly to form a 'transition' region between the neighbouring hard grains. Such a region may be viewed as behaving similarly to a region expanded from the grain boundary of the single-phased system. Note that the grain boundary (see figure 2(b)) in the single-phased system (of hard grains) is responsible for the remanence enhancement [19]. The soft grain, when inserted between two hard grains, then behaves like a massive grain boundary, resulting in significantly more enhancement.

More precisely, it is the abrupt changes of θ in the grain boundary of the single-phased system that made it less effective in enhancing remanence in contrast to the case for the composite system, where a gradual change in θ was noted. That this is so can be seen more clearly from the following section.

4. Integrated remanence enhancement

The reduced remanence of the soft phase M_r^s/M_S^s is obtained by averaging the quantity $M_S^s \cos\theta$ over the grain dimension of the soft phase, as well as over all possible easy-axis combinations α_1 and α_2:

$$M_r^s/M_S^s = \left(\int_{-\pi/2}^{\pi/2} \mathrm{d}\alpha_2 \int_{-\pi/2}^{\pi/2} \mathrm{d}\alpha_1 \int_{-L^s/2}^{L^s/2} M_S^s \cos\theta \, \mathrm{d}y\right) \Big/ \left(M_S^s L^s \int_{-\pi/2}^{\pi/2} \mathrm{d}\alpha_2 \int_{-\pi/2}^{\pi/2} \mathrm{d}\alpha_1\right) \tag{4.1}$$

where M_S^s is the saturation magnetization. With equation (3.14), this can be written as

$$M_r^s/M_S^s = \left(\int_{-\pi/2}^{\pi/2} \mathrm{d}\alpha_2 \int_{-\pi/2}^{\pi/2} \mathrm{d}\alpha_1 \frac{\sin(\delta^s/2)}{\delta^s/2} \cos[(\alpha_1 + \alpha_2)/2]\right) \Big/ \pi^2. \tag{4.2}$$

If all of the magnetic moments in the soft grain lie in the direction given by $\theta = (\alpha_1 + \alpha_2)/2$, then we have

$$M_r^s/M_S^s = \left(\int_{-\pi/2}^{\pi/2} \mathrm{d}\alpha_2 \int_{-\pi/2}^{\pi/2} \mathrm{d}\alpha_1 \cos[(\alpha_1 + \alpha_2)/2]\right) \Big/ \pi^2 = \frac{8}{\pi^2}. \tag{4.3}$$

Now, we can define a correction factor ξ to express the fact that the magnetic moments are not wholly aligned along the same direction (specified by $(\alpha_1 + \alpha_2)/2$), but point in various directions, so we may rewrite equation (4.2) as

$$M_r^s/M_S^s = \frac{8}{\pi^2}\xi. \tag{4.4}$$

In general, $\xi < 1$, but $\xi \to 1$ for very small L^s. Larger ξ simply reflects a slower and smoother change of θ in the soft phase, leading to larger enhancement. For our present composite system, the calculated reduced remanence enhancement of α-Fe, $(M_r/M_S)^{\alpha-\mathrm{Fe}}$, and ξ are given in figure 3. The figure shows that the reduced remanence is about 0.78 for 15 nm α-Fe grains, which is 22% more than the value 0.637 predicted from the S–W model for plane-isotropic grains. The figure reveals that the reduced remanence decreases with increasing grain size, which is in agreement with the experimental and numerical results.

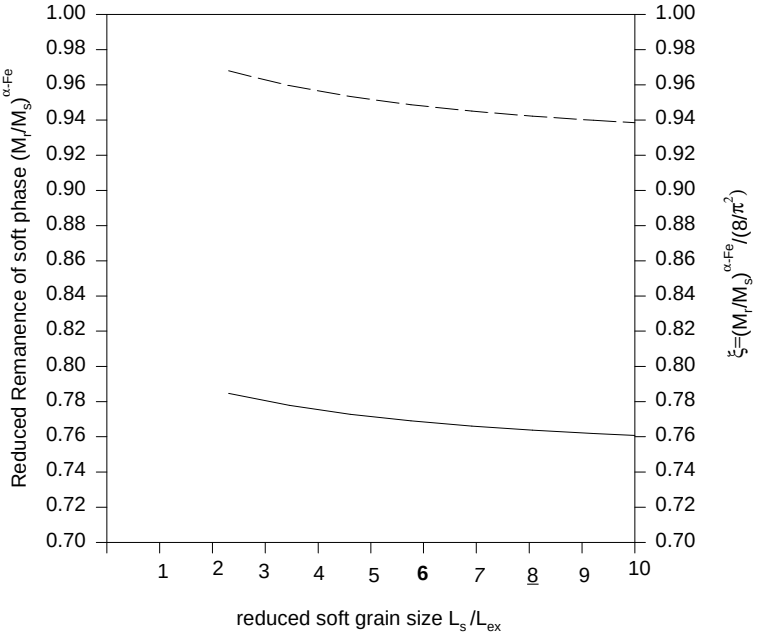

Figure 3. The reduced remanence $(M_r/M_S)^{\alpha-\mathrm{Fe}}$ and ξ as functions of L^s/L_{ex}, where $\xi = (M_r/M_S)^{\alpha-\mathrm{Fe}}/(8/\pi^2)$.

On the other hand, the remanence of the hard magnetic grain may be described by the S–W model. However, we shall ignore contributions from the grain boundaries as they are relatively small. According to the S–W model, the reduced remanence is 0.5 for three-dimensional-isotropic easy-axis distribution, and $2/\pi$ for plane-isotropic easy-axis distribution. Thus, we have

$$M_r^h/M_S^h = \frac{2}{\pi}. \tag{4.5}$$

The average remanence of a three-grain system (as shown in figure 1) may be obtained using the following expression:

$$M_r = \eta M_r^s + (1-\eta) M_r^h \tag{4.6}$$

where η is the percentage volume occupation of the soft-phased material. Substituting equations (4.4) and (4.5) into equation (4.6), we obtain

$$M_r = \frac{8}{\pi^2}\xi\eta M_S^s + (1-\eta)\frac{2}{\pi}M_S^h. \tag{4.7}$$

For composite materials with significant remanence enhancement, the soft-grain size should be less than half the domain wall width of the soft-phased material (which is ≈36.6 nm for α-Fe). In this size regime, ξ is nearly 1 (see figure 3). Thus, a good estimate for the remanence of composite materials with significant remanence enhancement can be obtained by setting $\xi = 1$ in equation (4.7), i.e.

$$M_r = \frac{8}{\pi^2}\eta M_S^s + (1-\eta)\frac{2}{\pi}M_S^h. \tag{4.8}$$

In figure 4, we show the calculated average remanence as a function of soft-phased grain size for two values of η. In the same figure, the results for the exchange-coupled single-phased $Nd_2Fe_{14}B$ and isolated $Nd_2Fe_{14}B$ grains are also given for comparison. It can be seen that remanence increases with volume occupation of the soft phase. For isolated $Nd_2Fe_{14}B$ grains, however, the remanence is $2M_S/\pi = 2(1.61)/\pi = 1.03$ T. Our previous work [19] has suggested that the maximum remanence enhancement is only 13% for exchange-coupled single-phased $Nd_2Fe_{14}B$ for a given size of 10 nm. This demonstrates that the remanence for composite systems can be enhanced through the inclusion of a soft phase, with the enhancement increasing with its volume occupation.

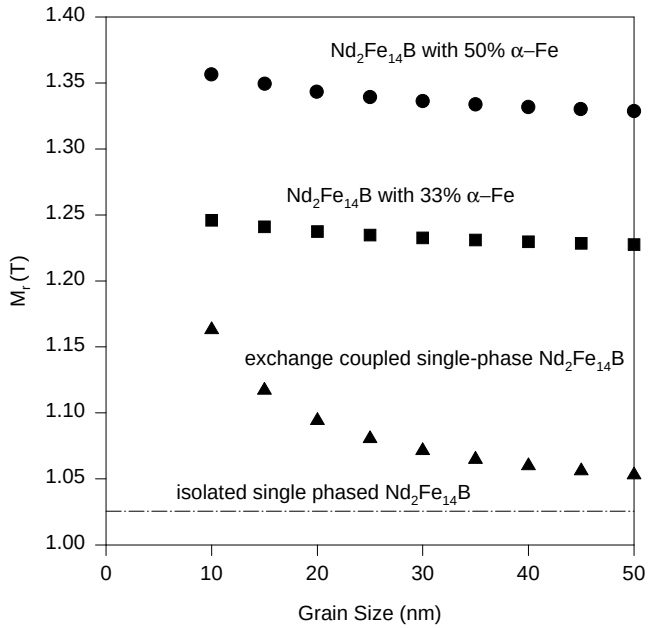

Figure 4. Remanence of the composite (α-Fe + Nd–Fe–B) system as a function of grain size for two α-Fe volume occupations.

In addition, the figure indicates that, although the remanence decreases with increasing grain size L^s, the change in the remanence is negligible. Similar results were also found by experiments [9], where it has been shown that, for a trilayer Nd–Fe–B/Fe/Nd–Fe–B system, the remanence takes a constant value for soft-grain sizes less than about 30 nm. Experiments have further indicated that the remanence varies approximately like $1/L^s$, for L^s in the region 40–110 nm. This, however, cannot be accounted for within our present model, as we have neglected the effects of the soft-grain anisotropy K^s, which can only be justified [4] if $L^s < \pi\Delta^s/2$.

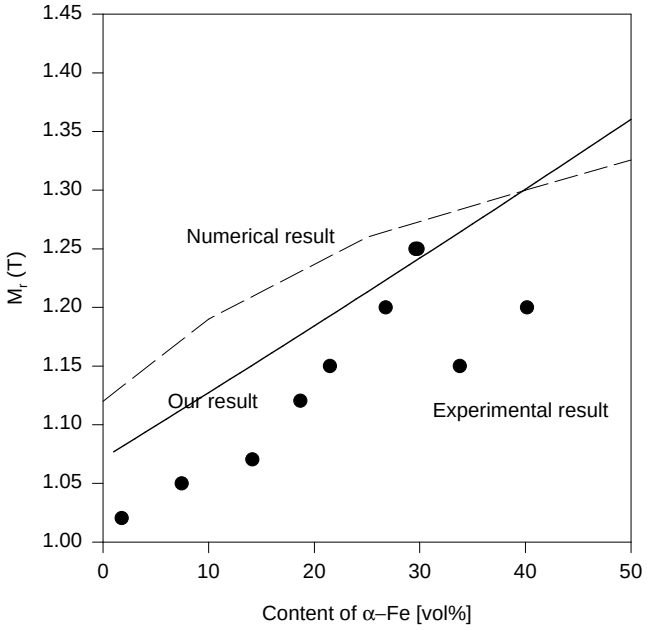

Figure 5. Variation of the remanence of the composite (α-Fe + Nd–Fe–B) system with the volume occupation η of the α-Fe phase. Experimental [8] (solid circles) and numerical [7] (long-dashed curve) results are shown for comparison. A grain size of 15 nm used in the present calculations was chosen to match the average size of reference [8], while a value of 20 nm was used in the numerical studies.

Figure 5 presents the calculated remanence according to equation (4.7) for a composite system with $L^s = 15$ nm, $L^h = 30$ nm, and $\xi = 0.96$, the latter being estimated from figure 3. Our results are in reasonable agreement with the experimental measurements. The overestimation, particularly for smaller volume occupation of the α-Fe, however, is due to our present model being plane isotropic rather than three-dimensionally isotropic as normally would be encountered in experiments. According to the S–W model, the remanence of the plane-isotropic easy-axis distribution is larger than that of the three-dimensional model, thus accounting for the discrepancy. Furthermore, we note that the experimental rate of increase of the remanence with the volume occupation of α-Fe, i.e. $\mathrm{d}M_r/\mathrm{d}\eta$, is generally larger than the slope of our calculated curve. This can be attributed to the fact that our model is one dimensional (where each grain has only two neighbouring grains) rather than three dimensional (where each grain has more than two neighbours), so there is an *underestimation* of the exchange interactions, and hence a smaller gradient.

The last point can be shown more explicitly as follows. Consider a three-dimensional (3D) system in which each and every cubic soft grain has, on average, n neighbouring hard

grains with easy axes α_i, $i = 1, 2, \ldots, n$. According to equation (3.15), it is reasonable to assume that the orientation θ_c of the magnetic moment at the centre of the soft grain in the remanent state can be written as

$$\theta_c = \left(\sum_{i=1}^{n} \alpha_i\right) \Big/ n. \tag{4.9}$$

To a good approximation, we may, following earlier discussions, assume that all magnetizations in the soft grain are oriented along this direction θ_c, so we can write the remanence for the soft grain as $M_r^s = M_S^s \cos\theta_c$. Supposing that the distribution of the easy axis is still plane isotropic, the average remanence contributed by the soft grain is then given by

$$\begin{aligned} M_r^s &= M_S^s \left(\int_{-\pi/2}^{\pi/2} \int_{-\pi/2}^{\pi/2} \cdots \int_{-\pi/2}^{\pi/2} \cos\theta_c \, \mathrm{d}\alpha_1 \, \mathrm{d}\alpha_2 \, \cdots \, \mathrm{d}\alpha_n \right) \Big/ \pi^n \\ &= M_S^s \left[\frac{\sin(\pi/2n)}{\pi/2n} \right]^n . \end{aligned} \tag{4.10}$$

Thus, for instance, assuming n to be 6, we get $M_r^s \approx 0.934 M_S^s$.

By differentiating equation (4.8) with respect to η, we get the gradient of the M_r–η plot for a one-dimensional (1D) composite system (figure 1) as

$$\left(\frac{\mathrm{d}M_r}{\mathrm{d}\eta}\right)_{1\mathrm{D}} = \frac{8}{\pi^2} M_S^s - \frac{2}{\pi} M_S^h. \tag{4.11}$$

Similarly, for the 3D grain distribution with $n = 6$, the corresponding expression is

$$\left(\frac{\mathrm{d}M_r}{\mathrm{d}\eta}\right)_{3\mathrm{D}} = 0.934 M_S^s - \frac{2}{\pi} M_S^h. \tag{4.12}$$

It is clear therefore that an extension into 3D for the grain distribution will result in a steeper slope, thereby bringing it into closer agreement with experiments. For sufficiently large η, on the other hand, the observed drop in remanence is expected since the average number of hard neighbouring grains would have decreased as some of these may have been replaced by soft ones.

5. Conclusions

The remanence enhancement of an isotropic nanostructured composite magnetic system has been discussed in detail. The magnetic moments in the soft-phased grains are exchange hardened by the neighbouring hard-phased grains so the remanence is enhanced. Although we have introduced a number of simplifications into our 1D model (e.g. the neglect of stray-field energy), our results are still in reasonable agreement with the experimental and numerical studies. The following conclusions can be reached:

(a) Firstly, remanence enhancement is largely dependent on the magnetic moment orientations in the soft-phased grains, so the smaller the soft grain and the larger the volume occupation of α-Fe, the greater the remanence enhancement.
(b) Secondly, although ξ is difficult to determine accurately, we have shown that ξ is nearly one for sufficiently small soft grains. Under this condition, a good and quick estimate for the remanence is provided by equation (4.8).
(c) Thirdly, as far as remanence enhancement is concerned, the soft grain in a composite system may be viewed as playing the same role as the grain boundary in the single-phased system, only more enhanced and effective.

References

[1] Buschow K H J 1988 *Ferromagnetic Materials* vol 4, ed E P Wohlfarth and K H J Buschow (Amsterdam: Elsevier) pp 1–130
[2] Kneller E F and Hawig R 1991 *IEEE Trans. Magn.* **27** 3588
[3] Skomski R and Coey J M D 1993 *Phys. Rev.* B **48** 15 812
[4] Leineweber T and Kronmüller H 1997 *J. Magn. Magn. Mater.* **176** 145
[5] Schrefl T, Fischer R, Fidler J and Kronmüller H K 1994 *J. Appl. Phys.* **76** 7053
[6] Fischer R, Kronmüller and Fidler J 1996 *J. Magn. Magn. Mater.* **153** 35
[7] Schrefl T, Fidler J and Kronmüller H K 1994 *Phys. Rev.* B **49** 6100
[8] Schrefl T, Schmidts H F, Fidler J and Kronmüller H K 1996 *J. Appl. Phys.* **80** 1667
[9] Parhofer S M, Wecker J, Kuhrt C, Gieres G and Schultz L 1996 *IEEE Trans. Magn.* **32** 4437
[10] O'Donnell K, Aindaw M, Harris I R, Skomski R and Coey J M D 1996 *J. Magn. Magn. Mater.* **157/158** 79
[11] Neu V, Klement U, Schäfer R, Eckert J and Schultz L 1996 *Mater. Lett.* **26** 167
[12] Wecker J, Schnitzke K, Cerva H and Grogger W 1995 *Appl. Phys. Lett.* **67** 563
[13] Liu J F and Davies H A 1996 *J. Magn. Magn. Mater.* **157/158** 29
[14] Ding J, McCormick P and Street R 1993 *J. Magn. Magn. Mater.* **124** 1
[15] Ding J, Liu Y, Street R and McCormick P 1995 *J. Magn. Magn. Mater.* **150** 329
[16] Ding J, Liu Y, Street R and McCormick P 1994 *J. Appl. Phys.* **75** 1032
[17] Hadjipanayis G C and Gong W 1988 *J. Appl. Phys.* **64** 5559
[18] Hu J F and Wang Z X 1995 *J. Phys.: Condens. Matter* **7** 8655
Hu J F and Wang Z X 1996 *J. Phys.: Condens. Matter* **8** 2243
[19] Zhao G P, Ong C K, Feng Y P, Lim H S and Ding J 1999 *J. Magn. Magn. Mater.* at press